Trends in CMIP5 Rainfall Patterns over Southwestern Australia

BHUPENDRA A. RAUT

School of Earth, Atmosphere and Environment, Monash University, Clayton, Victoria, Australia

MICHAEL J. REEDER AND CHRISTIAN JAKOB

Australian Research Council Centre of Excellence for Climate System Science, and School of Earth, Atmosphere and Environment, Monash University, Clayton, Victoria, Australia

(Manuscript received 8 August 2016, in final form 27 November 2016)

ABSTRACT

Previous work has shown that the sharp fall in winter rainfall over coastal southwestern Australia in the 1970s was mainly due to a fall in the frequency of fronts; the gradual reduction in rainfall since the late 1990s was due to a reduction in the number of light-rain days; and the increased inland summer rainfall in the 1970s was due to an increased number of easterly troughs. The current paper extends this earlier work by identifying the rainfall patterns in the region in 14 CMIP5 models for the period 1980–2005 and by calculating how these patterns are projected to change in the twenty-first century. The patterns are identified using *k*-means clustering of the rainfall, which are validated against observed rainfall clusters. Although the agreement between the models and the observation is generally good, the models underestimate the frequency of raining fronts. In both representative concentration pathway 4.5 and 8.5 (RCP4.5 and RCP8.5) scenarios the number of dry days increases significantly at the expense of light-rain days and frontal rainfall. However, these trends are twice as large in the RCP8.5 scenario as in the RCP4.5 scenario. The reduction in the rainfall from the historical period to the second half of the twenty-first century is produced mainly by a reduction in both the frequency and intensity of light rain and a reduction in the frequency of fronts in the westerlies.

1. Introduction

In the mid-1970s winter coastal rainfall in southwestern Australia (SWA) sharply fell (Nicholls et al. 1997; Hope et al. 2006), followed by a more gradual decline from the late 1990s onward. Summer rainfall, however, increased over the inland region of SWA in the mid-1970s (Fierro and Leslie 2013), although it too gradually declined after about 2000. The reduction in winter rainfall along the coast in the mid-1970s was linked to the poleward shift in the subtropical jet (Frederiksen and Frederiksen 2007), and Raut et al. (2014) showed that both the winter reduction along the coast and the increase in summer rainfall inland are associated with the positive phase of the southern annular mode (SAM). Moreover, they found that the earlier reduction in winter rainfall was due to fewer strong fronts, while the reduction in the late 1990s was due to an increase in dry days at the expense of light-rain days. They also found that the increase in summer rainfall was associated with more frequent and more intense easterly dips, which was possibly associated with the increase in the number of intense tropical cyclones in northwestern Australia (Nicholls et al. 1998; Kuleshov et al. 2008).

The future projections of rainfall from models of phase 5 of the Coupled Model Intercomparison Project (CMIP5) show that rainfall over the SWA will continue to decrease. In particular, many studies show a strong decrease in winter and spring rainfall in the projections, with these trends increasing with increasing greenhouse gases concentration (e.g., Pitman and Perkins 2008; Hope et al. 2015). Over SWA the CMIP5 models reproduce well the observed annual cycle of sea level pressure (SLP) (Hope et al. 2015), the spatial rainfall patterns (Irving et al. 2012), the seasonal cycle of rainfall (Moise et al. 2015), and the trends in the hemispheric circulation associated with these rainfall patterns (Frederiksen and Grainger 2015). However, a critical validation of the regional projections of rainfall is necessary given the incomplete description of the relevant physical processes in the CMIP5 models (Risbey and O'Kane 2011).

Corresponding author e-mail: Bhupendra A. Raut, bhupendra.raut@monash.edu

DOI: 10.1175/JCLI-D-16-0584.1

TABLE 1. Median rainfall in the historical runs for 1980–2005 of all models and the linear seasonal decadal trends for the RCP4.5 and RCP8.5 scenarios during 2006–99. The significant trends at 1% ($p < 0.01$) are marked in boldface, and those at 0.01% ($p < 0.0001$) are marked with an asterisk. (Expansions of acronyms are available online at http://www.ametsoc.org/PubsAcronymList.)

Dataset	Grid spacing	Median (mm day^{-1})	Linear trends in rainfall (mm day^{-1})							
			DJF		MAM		JJA		SON	
			RCP4.5	RCP8.5	RCP4.5	RCP8.5	RCP4.5	RCP8.5	RCP4.5	RCP8.5
Observation	0.05°	0.2	—	—	—	—	—	—	—	—
ACCESS1.0	1.25°	0.15	1.7	−1.7	0.82	−1.8	−2.2	**−4.1***	−1.4	**−2.7***
ACCESS1.3	1.25°	0.22	−2.2	**−2.8**	−2.1	**−5.3**	−0.92	**−6.3***	−0.94	**−2.2**
CanESM2	2.79°	0.31	3.6	2.1	−1.9	0.59	−1.5	**−4.5**	−0.18	−1.7
CMCC-CMS	1.86°	0.019	0.62	0.42	−0.45	−0.4	**−3.5**	**−8.7***	−0.48	**−1.9***
CNRM-CM5	1.4°	0.42	2.2	−2.3	−0.005	−0.44	−0.25	**−5.4**	−0.79	**−3.9***
CSIRO Mk3.0	1.86°	0.064	−1.3	−1.4	−1.8	−1.8	**−2.1**	**−2.5***	−1.8	**−1.8***
GFDL CM3	2.0°	0.17	−2.3	0.44	−4.7	−2.4	**−4.8***	**−7.1***	**−1.7**	**−2.0***
HadGEM2	1.25°	0.15	−0.81	−0.17	−0.17	−0.89	−1.6	**−5.0***	**−1.4**	**−2.1***
INM-CM4.0	1.5°	0.34	−1.2	−0.65	−1.2	−1.6	**−2.6**	**−2.9**	−0.93	−0.08
IPSL-CM5B	1.9°	0.088	−1.3	−0.53	0.53	0.81	**−4.4**	−3.8	−0.29	**−1.6**
MIROC5	1.4°	0.48	0.49	1.6	1.9	−0.89	−1.4	**−4.9**	−0.57	−0.24
MIROC-ESM	2.79°	0.49	−2	**−3.8**	−0.93	−1.3	−0.27	**−10***	−1.5	**−5.3***
MPI-ESM	1.86°	0.049	−1	−0.24	−0.57	**−5.2**	−1.9	**−7.7***	−0.08	**−2.9***
MRI-CGCM3	1.12°	0.18	−1.5	−2.2	−0.96	0.18	**−3.8**	**−6***	−0.49	−1.1
CMIP5 mean	—	—	−0.36	−0.81	−0.82	**−1.5**	**−2.2***	**−5.7***	**−0.9***	**−2.1***

Raut et al. (2014) showed that rainfall clustering is a useful method to identify the distinct synoptic patterns responsible for rainfall in SWA and to diagnose how changes in the rainfall are related to changes in the intensity and frequency of these synoptic patterns. The central aim of the present paper is to apply the clustering method to 14 CMIP5 models over the historical period and for representative concentration pathway 4.5 and 8.5 (RCP4.5 and RCP8.5) scenarios to understand how these synoptic patterns and the associated rainfall may change over the next century. We will also compare the key characteristics of regional rainfall patterns from models and observations in the CMIP5 historical runs. Nevertheless, this comparison is not a comprehensive verification of regional rainfall from the coupled general circulation models (GCM).

2. Data and methods

a. CMIP5 and ERA-I data

Rainfall observations for the period 1980–2005 are obtained from the Australian Water Availability Project (Raupach et al. 2009; Jones et al. 2009) in the form of daily gridded files. The CMIP5 (Taylor et al. 2012) data for 14 models for the historical period (1980–2005) and RCP4.5 and RCP8.5 projections (2006–99) are used. All the rainfall data are interpolated from their native resolution to a common grid with a 0.5° spacing (Table 1). The SLP fields for a larger domain around Western Australia are from the CMIP5 models and the European Centre for Medium-Range Weather Forecasts (ECMWF) interim reanalysis (ERA-Interim, hereafter ERA-I; Dee et al. 2011) for the period 1980–2005.

b. Clustering on rainfall

In this study we separated rain days for the cluster analysis, and the dry days were termed as the ''zeroth'' cluster. A rain day is one for which the daily mean rainfall, over land area in SWA, exceeds the median for the historical period in the observations or the model. As the median rainfall varies from model to model, the threshold for a rain day varies from model to model too (see Table 1 for medians). Defining a rain day this way ensures that, in the historical period, the number of rain days in each model is the same as in the observations. One consequence of this choice is that the so-called dry days in the models include many days with drizzle because of their well-documented tendency to produce too much light rain (Sun et al. 2006; Stephens et al. 2010).

The *k*-means algorithm of Anderberg (1973) is used to cluster rainy days in the historical period from observations and the CMIP5 models. In accordance with Raut et al. (2014), we used five clusters, as they represent major rain producing systems in the region, such as westerly fronts, easterly troughs, and cutoff lows. The model clusters are assumed to have a one-to-one correspondence with the observed clusters, and the Hungarian method (Hornik 2005) is used to assign model clusters to the observations by minimizing the Euclidean distance between the cluster centroids. This method is

found to work well except for clusters 3 and 5 for three models (ACCESS1.3, CanESM2, and CSIRO Mk3.0). Because of the similarity in the rainfall patterns and the poor simulations of strong fronts in these models, we swapped clusters 3 and 5 subjectively to put more coast-aligned rainfall in cluster 3 and the far inland pattern in cluster 5.

Future rain days from the CMIP5 projections are assigned to the historical clusters by calculating their Euclidean distances to the historical centroids. The historical median daily rainfall is again used to define a rain day so that changes in the frequency of rain days will be reflected in the change in the frequency of the clusters. In this way, the cluster frequencies and their trends from each model are comparable to each other in historical and future periods. Of course, to be useful, the model must reasonably simulate the observed rainfall patterns and should have a nonzero median rainfall.

c. *Trends and decomposition of change*

Linear decadal trends are computed for the rainfall and cluster frequencies, and their significance is tested with the Mann–Kendall p value (McLeod 2011). These trends are considered significant only at a 1% (p value < 0.01) level or better.

As in Raut et al. (2014), the change in rainfall of the ith cluster ΔR_i is attributed to a change in the intensity ΔP_i and change in frequency ΔN_i of the cluster through the equation

$$\Delta R_i = N_i \Delta P_i + P_i \Delta N_i + \Delta N_i \Delta P_i, \quad (1)$$

where N_i and P_i are the frequency and intensity of the ith cluster, respectively. The total rainfall change from all the clusters (k) can then be written as

$$\Delta R = \sum_{i=1}^{k} \Delta R_i. \quad (2)$$

The first and the second terms in Eq. (1) describe the change in rainfall due to intensity and frequency, respectively. The third term represents the second-order changes in rainfall resulting from the combination of changing intensity and frequency. This term was found to be negligible in all models when compared to the first two terms.

3. Results and discussion

a. *Rainfall patterns and seasonality*

The five clusters for the observed and CMIP5 rainfall in the historical period are shown in Fig. 1 with their composite SLP patterns shown in Fig. 2. The models reproduce the coastal and inland rainfall patterns with varying degrees of skill.

Physically, cluster 1 describes light rainfall produced in the midlatitude westerlies. It is the most frequent pattern of rainfall, occurring around one-third of the time in the ERA-I and the models. Cluster 2 describes the rainfall associated with the passage of a front or trough in the westerlies. The rainfall in this cluster is mostly confined to the coast. All but two models (ACCESS1.3 and INM-CM4.0) reproduce the correct pattern of SLP associated with this rainfall pattern.

Heavy rainfall associated with a strong front and cutoff low is represented by cluster 3 in the observations. However, the models' versions of this pattern show the most variation of the five clusters, making it difficult to assign to it a single synoptic type. For this reason, the cluster is called here the ''assorted troughs.'' In contrast to observations, this pattern of rainfall is populated by cutoff lows (e.g., IPSL-CM5B) and troughs (e.g., CanESM2) in the easterlies in all the models except CMCC-CMS. This is consistent with a shift in the centers of the heavy precipitation to the southern coast and farther inland than observed. Moreover, in models where the maximum of rainfall in cluster 3 is nearer to the west coast (e.g., CMCC-CMS), the westerly trough is visible. A cutoff low is present in the models where the rainfall maximum is stretched inland toward the southeast (e.g., HadGEM2). As mentioned in section 2b, ACCESS1.3, CanESM2, and CSIRO Mk3.0 have the largest discrepancies from the observed cluster 3 in Euclidean space.

Clusters 4 and 5 describe inland rainfall associated with troughs in the easterlies. The heavier rainfall in cluster 5 is mostly associated with a deeper trough. The rainfall and SLP associated with the clusters is well represented by the models, although many models overestimate the frequency of cluster 4. Note that, although in the models, cluster 3 is also associated with an easterly trough, clusters 4 and 5 are synoptically different from cluster 3 because of the location of rainfall and the weak westerly trough to the south instead of a ridge. This also indicates the presence of cutoff lows in the cluster 3.

The monthly frequency and intensity of each cluster in the historical period are shown in Fig. 3. In clusters 1, 2, and 4 (the light rain, westerly front, and easterly trough clusters, respectively) the progression of the model mean follows that of the observations reasonably well. However, fronts are underestimated throughout May–October. The model frequencies that agree least well with observations are those of clusters 3 and 5 (assorted troughs and strong easterly trough cluster, respectively),

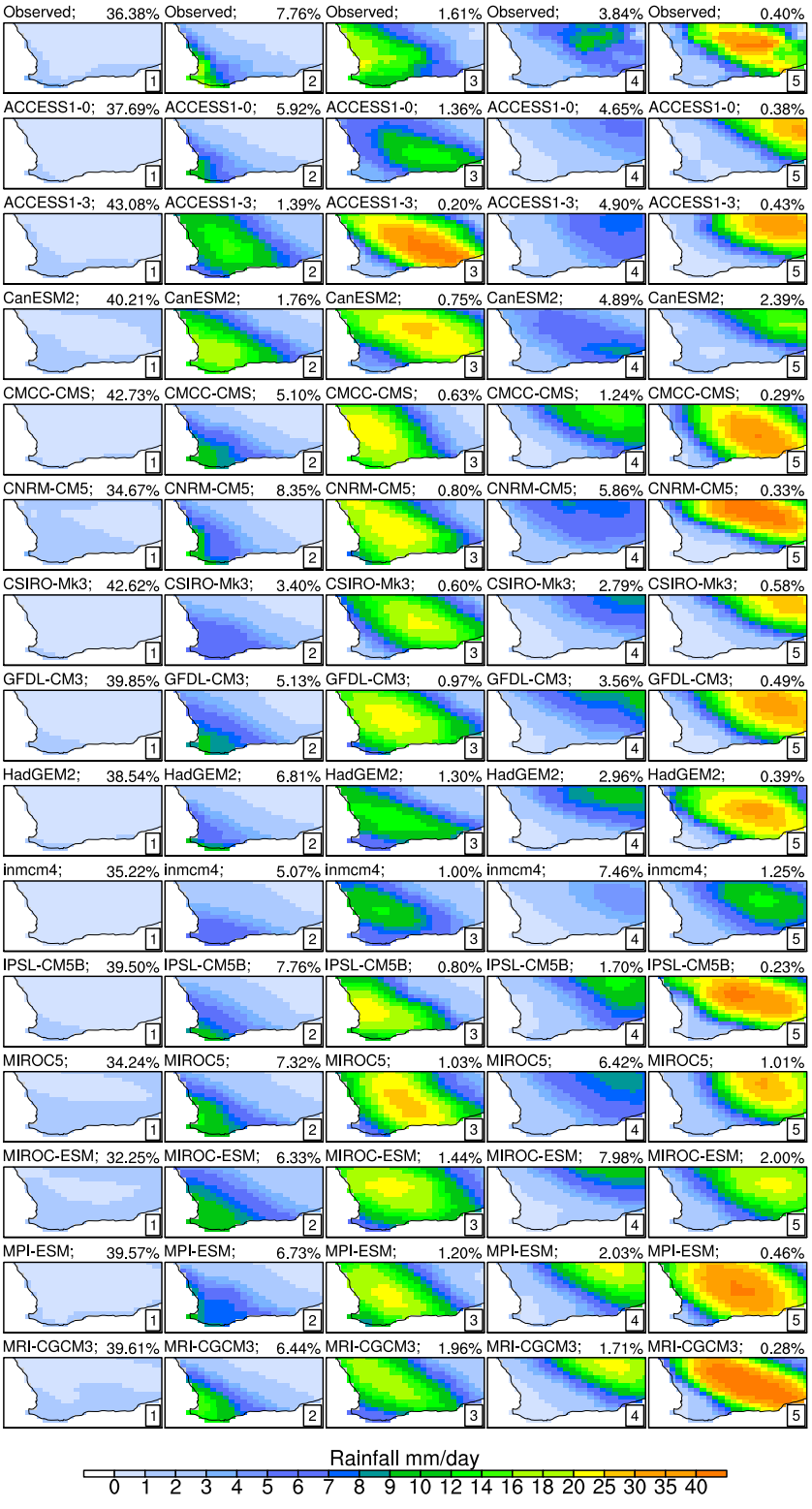

FIG. 1. (left)–(right) Five rainfall clusters for (top)–(bottom) the observed data and the 14 CMIP5 models for the historical period (1980–2005). The frequency of occurrence of clusters is shown at the top-right corner of each panel. Considering their pressure patterns in Fig. 2, these patterns are numbered as follows: 1) light rain, 2) westerly front, 3) assorted troughs, 4) easterly troughs, and 5) strong easterly troughs.

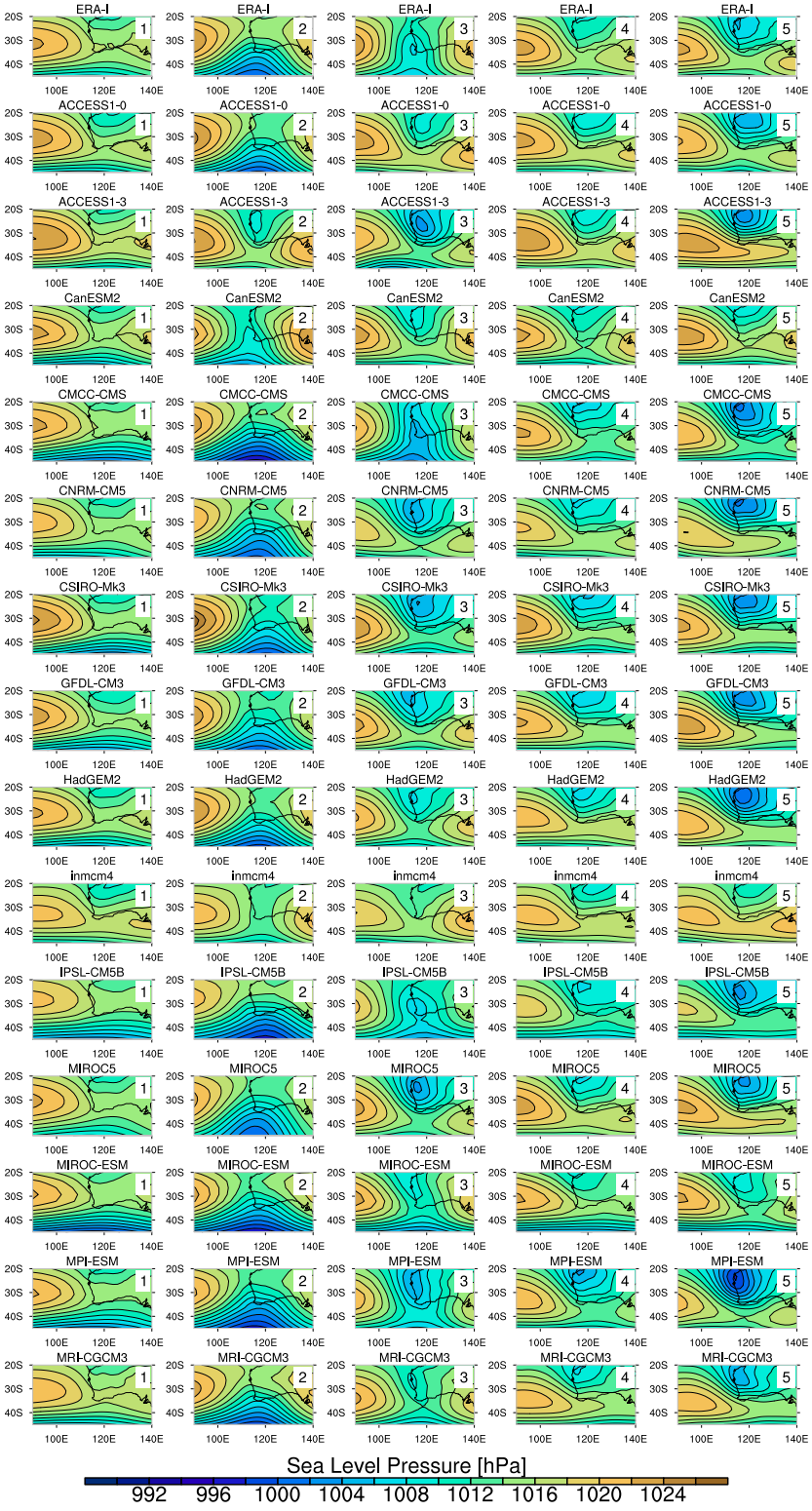

FIG. 2. Average SLP patterns associated with the five rainfall clusters shown in Fig. 1. (top)–(bottom) The SLP patterns for the observed clusters from ERA-I and the CMIP5 models.

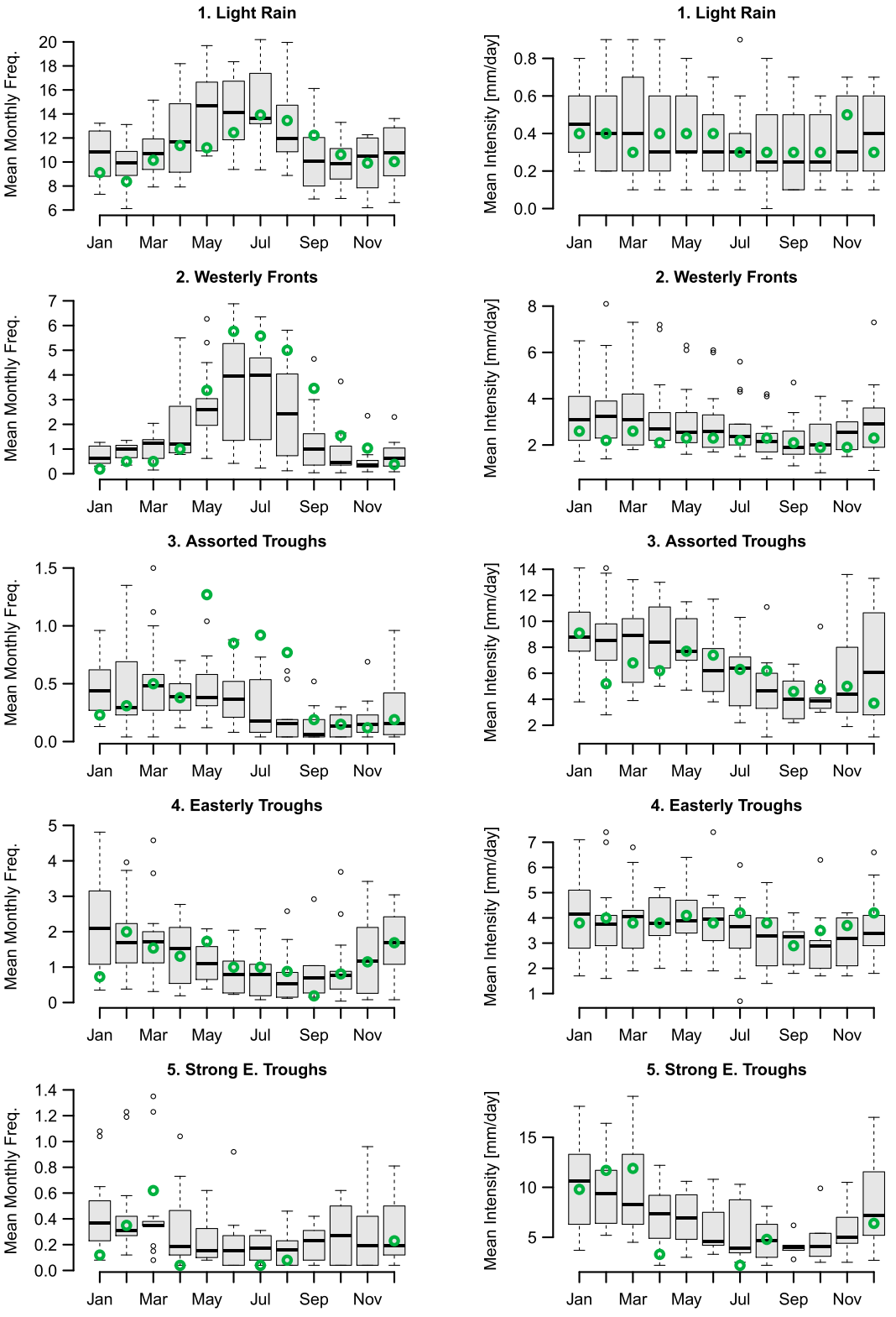

FIG. 3. (left) Mean monthly frequency and (right) mean intensity of (top)–(bottom) the five clusters for the historical period (1980–2005). The CMIP5 models are shown by the box-and-whisker plots, and observed data are shown by green circles.

which are also the least frequent clusters. In the case of the frequency of cluster 3 in winter, observations lie well above the interquartile range of the models, which presumably reflects the fact that cluster 3 is dominated by westerly fronts, easterly troughs, or cutoff lows, depending on the model. The frequency of cluster 3 is well simulated for the transition period (February–April) when cutoff lows are dominant over the region (Pook et al. 2012).

b. Overall trends in future rainfall

The seasonal trends in the rainfall for the multimodel mean and each individual model are listed in Table 1. The linear rainfall trends in the ensemble mean in all seasons are negative, and their magnitudes are about twice that in the RCP8.5 scenario compared with RCP4.5. There is no significant trend in the ensemble mean in DJF in either scenario, while in MAM the trend becomes significant at the 1% level in RCP8.5. The strongest trends in the ensemble mean are in JJA (-2.2 and $-5.7\,\mathrm{mm\,day^{-1}}$), followed by SON ($-0.89$ and $-2.1\,\mathrm{mm\,day^{-1}}$), which are both significant to 0.01% in both scenarios.

The trends in the ensemble means are more significant than those for the individual models as a result of decreased variability in the time series of the ensemble mean. The rainfall trend is negative in all models in JJA and SON for both the RCP4.5 and RCP8.5 scenarios. For RCP4.5, 6 of the 14 models have significant trends in JJA, whereas only 2 models have significant trends in SON. On the other hand, for RCP8.5, 13 and 10 models have significant trends in JJA and SON, respectively. In DJF and MAM, however, the sign of the trend is mixed, with no model having a significant trend for RCP4.5 and only two models having significant trends in both seasons for RCP8.5.

c. Trends in the rainfall patterns

Notwithstanding the discrepancies between the observations and the models in the least frequent clusters, overall the model clusters agree reasonably well with the observed clusters and can be used to identify distinct synoptic patterns associated with rainfall in the region. The trends in the cluster frequency for the historical and projection periods are shown in Fig. 4. As expected the RCP4.5 and RCP8.5 scenarios follow the same path in the early part of the twenty-first century but diverge in the latter half of the century. For example, taken over the whole projection period, the trends in RCP8.5 are more than double for clusters 0, 1, and 2. The trends in the historical runs are not significant because of a shorter period.

In the projections, dry days increase significantly in both scenarios with up to two-thirds of the increase in dry days compensated by the reduction in light-rain days (cluster 1). In RCP4.5, 1.7 dry days are added every decade, although the trend flattens in the latter half of the century. In RCP8.5, the increase in dry days continues at the rate of 4 days $\mathrm{decade^{-1}}$, from approximately 180 days $\mathrm{yr^{-1}}$ currently to 220 days $\mathrm{yr^{-1}}$ by the end of the century.

Around a quarter of the increase in dry days comes from a decrease in the frequency of westerly fronts (cluster 2). A reduction of close to 1 front every decade in RCP8.5 and half that in RCP4.5 are projected. By the end of the century, the annual frequency of westerly fronts in the models falls from 20 to 16 and 11 in RCP4.5 and RCP8.5, respectively, although it should be noted that the models underestimate the frequency of the westerly fronts. The reduction in easterly troughs (cluster 4) is significant in both the scenarios, although for strong troughs (cluster 5) only the negative trend in the RCP8.5 scenario is significant. Note that strong troughs only occur in summer, and models are unable to produce the annual cycle of this cluster.

d. Decomposition of the rainfall changes

This section investigates the contribution from each cluster to SWA rainfall changes. To do so, the change in the annual cluster rainfall from the historical period to the second half of the twenty-first century is decomposed into the change resulting from changes in intensity and that resulting from changes in the frequency of each cluster (Fig. 5). The reduction in light rain (cluster 1) is large in both scenarios, with all the models agreeing on the sign of the intensity and frequency changes. The total change in light rainfall arises from both a reduction in frequency and intensity. However, when the intensity of the light rain falls to below the threshold value (the median in the historical period), it is classified as a dry day. In most models the reductions due to intensity and frequency are almost doubled in the RCP8.5 compared with RCP4.5.

The reduction in rainfall from the westerly fronts (cluster 2) is mostly due to a reduction in its frequency. There is a slight increase in the intensity of the rainfall associated with westerly fronts, although this is offset by even larger changes in rainfall resulting from decreases in their frequency. The increase in intensity is largest in MIROC5.

The changes in the rainfall due to the intensity of easterly troughs (cluster 4) and strong easterly troughs (cluster 5) are small, with no consistent sign from model to model. Likewise, for the rainfall changes associated

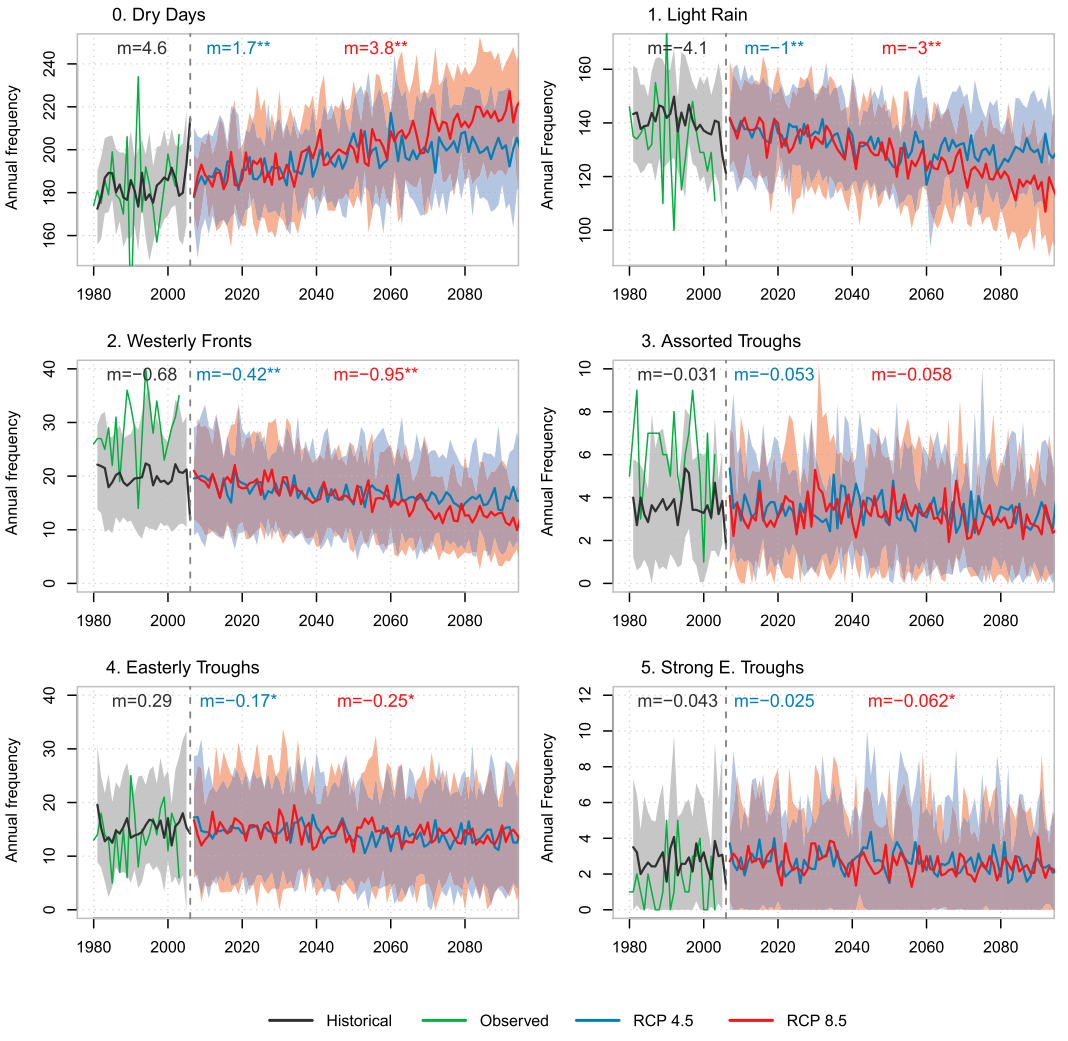

FIG. 4. Annual frequency of dry days and the five rainfall clusters for the historical period (1980–2005) and for RCP4.5 (blue) and RCP8.5 (red) scenarios (2006–99). The shadings cover one standard deviation (1σ) from model mean. Decadal trends and their significance for historical and projection periods are shown at the top of each panel. The trends significant at 1% are shown with a single asterisk and those at 0.01% are shown with two asterisks.

with assorted troughs (cluster 3), the changes due to frequency and intensity do not show clear or consistent trends. This could be a result of the presence of various weather systems in the cluster.

4. Conclusions

Rainfall clusters and their associated synoptic patterns for regional rainfall over SWA (in a 7° × 10° domain) from 14 CMIP5 models were calculated and compared against the analogous rainfall clusters and synoptic patterns from observation. Rainfall clustering has been shown to be a useful method to: (i) identify the distinct synoptic patterns responsible for rainfall in SWA, and (ii) diagnose how projected changes in the rainfall are related to changes in the intensity and frequency of these synoptic patterns. We found that all the significant rainfall trends over the region are sensitive to the greenhouse gas emissions scenario. The key conclusions of the study are summarized below:

- Despite the relatively coarse resolution (1.1°–2.8°) and the limitations of GCMs in representing regional processes, the CMIP5 models reproduce the observed coastal and inland rainfall patterns over SWA. The models also reproduce the associated pressure patterns and the seasonal cycle for each cluster. An exception is cluster 3, which has diverse weather systems in the models.

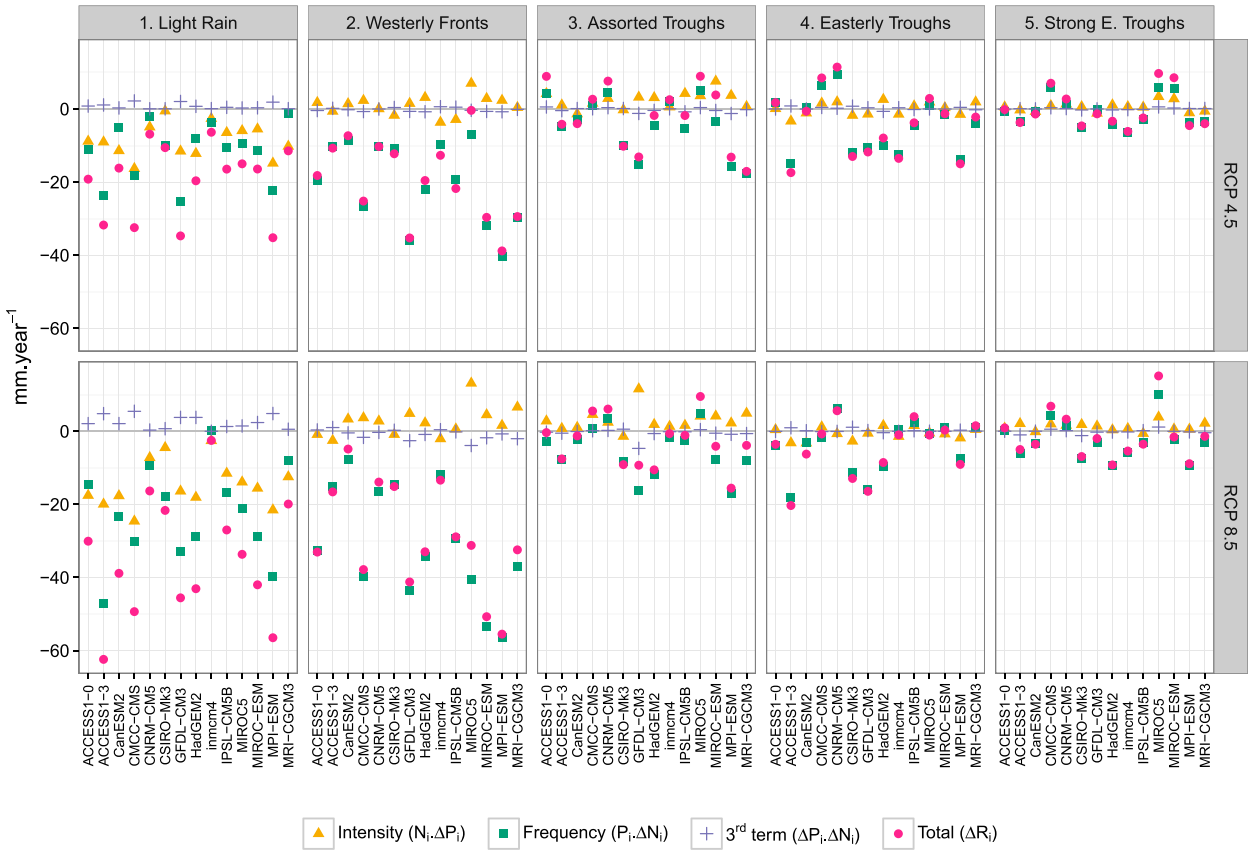

FIG. 5. Contribution to the total change in mean annual rainfall from the change in the intensity and the change in the frequency of (left)–(right) the five clusters for the (top) RCP4.5 and (bottom) RCP8.5 scenarios. The change is computed from the historical period (1980–2005) to the latter half of the projection period (2052–99), applying Eq. (1) to the 14 CMIP5 models.

- Frequency of frontal rain is underestimated in the historical period, and strong fronts are rare in all the CMIP5 models.
- The strongest trends in the model ensemble mean rainfall are in JJA (-2.2 and $-5.7\,\mathrm{mm\,day^{-1}}$) and SON ($-0.89$ and $-2.1\,\mathrm{mm\,day^{-1}}$), which are both significant to 0.01% in both the scenarios.
- The projected drying is due mainly to a decrease in frequency and intensity of light-rain days and fewer occurrences of westerly fronts, the effect of which is more pronounced in RCP8.5 than RCP4.5 scenarios.
- The frequency of easterly troughs is likely to reduce at $0.25\,\mathrm{decade^{-1}}$ in RCP8.5 as opposed to positive trends in the historical period.

Like Polade et al. (2014), the present study finds that the frequency of dry days increases significantly. The dry days are associated with a more persistent subtropical ridge over the region, which is consistent with an expansion of the Hadley cell (Seidel et al. 2008; Choi et al. 2014; Schwendike et al. 2015).

Raut et al. (2014) found that in the past the wintertime rainfall over SWA decreased because of a decreased frequency in fronts and showed that this is consistent with a positive trend in the SAM (implying a poleward shift in the storm track). This trend in SAM is projected to continue under the RCP8.5 scenario (Gillett and Fyfe 2013; Frederiksen and Grainger 2015) and the rainfall changes found in the present study are consistent with the projected trend in SAM.

Acknowledgments. This work received funding from the Cooperative Research Centre for Water Sensitive Cities Projects B1.1 and B1.3 and the Australian Research Council Centre of Excellence for Climate System Science (CE110001028). The R programming language (http://www.R-project.org), NCAR Command Language (NCL; http://dx.doi.org/10.5065/D6WD3XH5), and Climate Data Operators (CDO) were used for data analysis and graphics. We acknowledge the World Climate Research Programme's Working Group on Coupled Modelling, which is responsible for CMIP, and we

thank the climate modeling groups for producing and making available their model output. For CMIP the U.S. Department of Energy's Program for Climate Model Diagnosis and Intercomparison provides coordinating support and led development of software infrastructure in partnership with the Global Organization for Earth System Science Portals. Lam Hoang is thanked for collecting CMIP5 data. We are grateful to James Risbey and an anonymous reviewer for their insightful comments that helped improve the manuscript.

REFERENCES

Anderberg, M., 1973: *Cluster Analysis for Applications.* Academic Press, 359 pp.

Choi, J., S.-W. Son, J. Lu, and S.-K. Min, 2014: Further observational evidence of Hadley cell widening in the Southern Hemisphere. *Geophys. Res. Lett.*, **41**, 2590–2597, doi:10.1002/2014GL059426.

Dee, D., and Coauthors, 2011: The ERA-Interim reanalysis: Configuration and performance of the data assimilation system. *Quart. J. Roy. Meteor. Soc.*, **137**, 553–597, doi:10.1002/qj.828.

Fierro, A. O., and L. M. Leslie, 2013: Links between central west Western Australian rainfall variability and large-scale climate drivers. *J. Climate*, **26**, 2222–2246, doi:10.1175/JCLI-D-12-00129.1.

Frederiksen, C. S., and S. Grainger, 2015: The role of external forcing in prolonged trends in Australian rainfall. *Climate Dyn.*, **45**, 2455–2468, doi:10.1007/s00382-015-2482-8.

Frederiksen, J. S., and C. S. Frederiksen, 2007: Interdecadal changes in Southern Hemisphere winter storm track modes. *Tellus*, **59A**, 599–617, doi:10.1111/j.1600-0870.2007.00264.x.

Gillett, N., and J. Fyfe, 2013: Annular mode changes in the CMIP5 simulations. *Geophys. Res. Lett.*, **40**, 1189–1193, doi:10.1002/grl.50249.

Hope, P., W. Drosdowsky, and N. Nicholls, 2006: Shifts in the synoptic systems influencing southwest Western Australia. *Climate Dyn.*, **26**, 751–764, doi:10.1007/s00382-006-0115-y.

——, and Coauthors, 2015: Southern and south-western flatlands cluster report. CSIRO Rep., 64 pp.

Hornik, K., 2005: A clue for cluster ensembles. *J. Stat. Software*, **14**, doi:10.18637/jss.v014.i12.

Irving, D. B., P. Whetton, and A. F. Moise, 2012: Climate projections for Australia: A first glance at CMIP5. *Aust. Meteor. Oceanogr. J.*, **62**, 211–225.

Jones, D., W. Wang, and R. Fawcett, 2009: High-quality spatial climate data-sets for Australia. *Aust. Meteor. Oceanogr. J.*, **58**, 233–248.

Kuleshov, Y., L. Qi, R. Fawcett, and D. Jones, 2008: On tropical cyclone activity in the Southern Hemisphere: Trends and the ENSO connection. *Geophys. Res. Lett.*, **35**, L14S08, doi:10.1029/2007GL032983.

McLeod, A., 2011: Kendall: Kendall rank correlation and Mann–Kendall trend test, version 2.2. R package. [Available online at https://CRAN.R-project.org/package=Kendall.]

Moise, A., and Coauthors, 2015: Evaluation of CMIP3 and CMIP5 models over the Australian region to inform confidence in projections. *Aust. Meteor. Oceanogr. J.*, **65**, 19–53.

Nicholls, N., L. Chambers, M. Haylock, C. Frederiksen, D. Jones, and W. Drosdowsky, 1997: Climate variability and predictability for south-west Western Australia. Bureau of Meteorology Research Centre Phase 1 Rep. to the Indian Ocean Climate Initiative, 52 pp.

——, C. Landsea, and J. Gill, 1998: Recent trends in Australian region tropical cyclone activity. *Meteor. Atmos. Phys.*, **65**, 197–205, doi:10.1007/BF01030788.

Pitman, A., and S. Perkins, 2008: Regional projections of future seasonal and annual changes in rainfall and temperature over Australia based on skill-selected AR4 models. *Earth Interact.*, **12**, 1–50, doi:10.1175/2008EI260.1.

Polade, S. D., D. W. Pierce, D. R. Cayan, A. Gershunov, and M. D. Dettinger, 2014: The key role of dry days in changing regional climate and precipitation regimes. *Sci. Rep.*, **4**, 4364, doi:10.1038/srep04364.

Pook, M. J., J. S. Risbey, and P. C. McIntosh, 2012: The synoptic climatology of cool-season rainfall in the Central Wheatbelt of Western Australia. *Mon. Wea. Rev.*, **140**, 28–43, doi:10.1175/MWR-D-11-00048.1.

Raupach, M. R., P. Briggs, V. Haverd, E. King, M. Paget, and C. Trudinger, 2009: Australian Water Availability Project: CSIRO Marine and Atmospheric Research component: Final report for phase 3. CAWCR Tech. Rep. 13, 67 pp. [http://www.csiro.au/awap/doc/CTR_013_online_FINAL.pdf.]

Raut, B. A., C. Jakob, and M. J. Reeder, 2014: Rainfall changes over southwestern Australia and their relationship to the southern annular mode and ENSO. *J. Climate*, **27**, 5801–5814, doi:10.1175/JCLI-D-13-00773.1.

Risbey, J. S., and T. J. O'Kane, 2011: Sources of knowledge and ignorance in climate research. *Climatic Change*, **108**, 755–773, doi:10.1007/s10584-011-0186-6.

Schwendike, J., G. J. Berry, M. J. Reeder, C. Jakob, P. Govekar, and R. Wardle, 2015: Trends in the local Hadley and local Walker circulations. *J. Geophys. Res. Atmos.*, **120**, 7599–7618, doi:10.1002/2014JD022652.

Seidel, D. J., Q. Fu, W. J. Randel, and T. J. Reichler, 2008: Widening of the tropical belt in a changing climate. *Nat. Geosci.*, **1**, 21–24, doi:10.1038/ngeo.2007.38.

Stephens, G. L., and Coauthors, 2010: Dreary state of precipitation in global models. *J. Geophys. Res.*, **115**, D24211, doi:10.1029/2010JD014532.

Sun, Y., S. Solomon, A. Dai, and R. W. Portmann, 2006: How often does it rain? *J. Climate*, **19**, 916–934, doi:10.1175/JCLI3672.1.

Taylor, K. E., R. J. Stouffer, and G. A. Meehl, 2012: An overview of CMIP5 and the experiment design. *Bull. Amer. Meteor. Soc.*, **93**, 485–498, doi:10.1175/BAMS-D-11-00094.1.